IASJ
المجلات الاكاديمية العراقية
Journal of Kufa for Chemical Sciences
ISSN(P) :2077-2351 ISSN(E): 3006-3280
Journal Homepage:
https://journal.uokufa.edu.iq/index.php/jkcs/index

Article

Thermodynamic Study of Cadmium Ions Removal from Aqueous Solution using Spherical Alumina and Zeolite Alumina Nanocomposite

Walaa Abdul Zahra Jafar Abas **Majida Hameed Khazaal**

Department of Chemistry-Factually of Education for Girls-University of Kufa-Iraq

majidah.alkhazaali@uokufa.edu.iq

https://orcid.org/my-orcid?orcid=0000-0002-3156-5632

Abstract

Cd (II) is among the most hazardous transition metals for biological species Due to its cumulative toxicity and its effect on the kidneys and vital tissues. Consequently, it is imperative to develop effective strategies for the remediation of cadmium from water and soil. Spherical alumina and zeolite alumina nanocomposites have been investigated theoretically and empirically for their efficacy in removing Cd ions from their aqueous solution. Various advanced techniques, such as X-ray diffraction, scanning electron microscopy (SEM-EDS), Fourier Transform Infrared Spectroscopy (FT-IR), and (BET) surface area analysis, were utilized to examine the crystalline, morphological, chemical, and porosity properties of adsorbents. Optimal Cd(II) removal occurred at pH 6, and the efficiency was influenced by both the initial Cd(II) concentration and the alumina content in the adsorbents. The sorption of Cd ions on spherical alumina exhibited a higher removal efficiency due to their high surface area and active sites, that achieved a removal efficiency of 92.5%, compared to 90% of zeolite-alumina nanocomposite with multilayer adsorption capacities of 3.07 mg/g and 8.95 mg/g, respectively. The collected

experimental adsorption data were analysed using five isotherm models. The Freundlich, Dubinin, and Temkin adsorption isotherm models yielded the most accurate fit for the Cd (II) ions adsorption data, indicating that the adsorption process is multilayered. The obtained thermodynamic values demonstrated that the adsorption process is spontaneous and exothermic on the zeolite-alumina nanocomposite with decreased randomness in contrast to spherical alumina at the solid adsorbents –ions adsorbate interface during the adsorption process.

Keywords: heavy metals; Aluminium oxide; Nanocomposites; Adsorption; Removal

1-Introduction

Heavy metal contamination represents the foremost concern in the global assessment of drinking water quality. Due to its toxicity, bioaccumulation, and lack of biodegradability, using this contaminated water can have catastrophic consequences for communities and individuals [(1)]. In recent years, several adsorbents, such as agricultural waste, leaf powder from Lycopersicon esculentum, tea waste, microorganisms, yeast, and red mud, have been employed to remove heavy metals from wastewater. Because of their improved adsorption properties, nanomaterials are used for heavy metal contamination removal [(2)]. Bimetallic nanocomposites have a larger surface area than their monometallic counterparts, which increases their adsorption capacity [(3)]. Cadmium ions are often considered among the most detrimental pollutants in the ecosystem. They can permeate soil and aquatic environments via the electroplating industry, battery manufacturing, plating procedures, fertilizers, insecticides, dyes, and alloy production [(3,4)]. The elimination of these toxins is a burgeoning area of research and a pressing necessity in environmental science. Researchers have devised numerous methods for the remediation of wastewater from heavy metals, including precipitation, ion exchange, filtration, membrane separation, coagulation, and adsorption [(5, 6)]. Numerous ways are costly, each possessing distinct advantages and downsides.

Among the methods for heavy metal removal from wastewater, adsorption is one of the most often employed and effective techniques relative to other processes [7]. Recently, researchers dedicated considerable work to the study of nano-adsorbents. These are materials possessing nanoscale characteristics utilized for the removal of molecules from liquids or gasses [8]. Nanomaterials function as attractive adsorbents owing to their large surface area and distinctive physical and chemical characteristics. Consequently, researchers are developing nano-adsorbents with specific functionalization to enhance adsorption selectivity [9, 10]. Reversible base-exchange reactions can be carried out using zeolites, which are inexpensive and crystalline tectosilicate adsorbents. Mixing certain amounts of feldspar, clay, and soda ash was the traditional method for synthesizing zeolites [11]. Due to their many useful properties, such as being inexpensive, naturally occurring, thermally stable, selective, and having a small-pore structure with a large specific surface area [12,13] zeolites are used in many different contexts. They are catalytic agent [14, 15] ion exchangers [16], airborne purifiers [17], and adsorbents surfaces for inorganic materials [18,19]. However, they have a limited capacity to absorb cationic contaminants [20]. Natural zeolites can be changed by inorganic substances to make them better at absorbing heavy metal ions and organic pollutants [21]. Zeolites have a three-dimensional structure made of SiO□ and AlO□ tetrahedra [22]. The aluminium or silicon ion occupies the core of the tetrahedron, while oxygen atoms are positioned at the four vertices. The substitution of Si□□ with Al□³ induces a negative charge in the lattice, which is neutralized by exchangeable cations such as sodium, potassium, or calcium [23]. The monoethanolamide modification of zeolite improved its CO_2 absorption capacity relative to the raw zeolite. Researchers recorded the removal of amoxicillin from wastewater using modified zeolite-MgO [24]. The adsorption characteristics of $C_{22}H_{24}N_2O_9.ClH$ on magnetic zeolite/Fe□O□ nanoparticles exhibited the superparamagnetic features of zeolite/Fe□O□, facilitating the effective adsorption of oxytetracycline hydrochloride [25]. Efficient treatment methods, including adsorption technologies for water purification, are

essential to alleviate the detrimental effects that toxic metals—such as cadmium, chromium, lead, mercury, and nickel—impose on human health and ecosystems [26]. Recently, nanoscale materials presented a compelling approach for the removal of hazardous metals from aquatic ecosystems. Al□O□ nanoparticles are a significant oxide mineral in geological settings and are extensively utilized as sorbents and catalysts in many chemical processes in aqueous environments [27]. The acidic and basic properties of alumina are the principal drivers driving its widespread applications. Consequently, aluminium oxide is pivotal in the adsorption process as it enhances the aggregation of adsorbate ions on solid surfaces.

The main goal of this study is to find out how adding aluminium oxide to zeolite affects the removal of cadmium ions from aqueous solutions by developing effective and cost-effective adsorbents, particularly for wastewater applications. To our knowledge, this is the first time that zeolite modified with aluminium oxide nanoparticles has been reported and tested as a nanocomposite for cadmium ion removal from synthetic wastewater. The shape, structure, chemical composition, surface area and particle size of the doped zeolite were also examined. The experimental results were examined using Freundlich, Langmuir, Temkin, Harkin-Gora, and Dubinin adsorption isotherm models, along with thermodynamic values.

2. Practical Methods

2.1. Materials description and preparation methods

Sigma-Aldrich provided all high-purity chemicals that were used without further processing. Al(NO□)□ · 9H□O (99.99%), Cd(NO□)□·4H□O (99.9%), NaOH (98.0%), HCl (99.8%), and C□H□OH (99.50%). At room temperature, 10 g of zeolite were weighed out and mixed with 100 ml of a solution that had 2 wt.% Al (NO□)□ · 9H□O, at ambient temperature. The resultant mixes were agitated vigorously for 30 minutes and thereafter transferred to autoclaves. The spacemen subjected the specimens to a temperature of 180°C for 24 hours before allowing them to cool to ambient temperature. The product was centrifuged at 4000 rpm for

15 minutes and then washed several times with ultrapure water. The sample was calcined at a rate of 2°C/min until it reached 500°C to eliminate any moisture or hydroxide integrated into the structure.

2.2. Adsorbent Characterization

The chemical characteristics of adsorbents were analysed using FTIR (Shimadzu, Japan), BET (Quantachrome Autosorb-1), SEM (Hitachi TM3000), EDS (Bruker Quantax 70 EDS system), and XRD (Bruker D8 Advance). The Brunauer Emmett Teller (BET) method is used to calculate the adsorbents' specific surface area and pore porosity by nitrogen gas as adsorbent. About 200 mg of samples were heated to 350°C in a vacuum for 5 hours. The pore diameter and pore volume were obtained using Barrett Joyner Halenda (BJH) models. The crystal structure of the adsorbent samples was characterized by X-ray diffraction (Shimadzu XRD 6000) measurements that were performed on a Bruker diffractometer with a CuKα radiation source (λ = 1.5406Å) and the X-ray intensities were recorded every 0.027° step from 0° to 80°. The diffractometer works at 40 kV with a step-scan time of 4 s. These absorbents were described by their morphologies and structures using a Hitachi TM3000 scanning electron microscope at a voltage of 20 kV and magnifications of up to 100X, along with a Bruker Quantax 70 EDS system for elemental analysis.

2.3. Cd^{+2} adsorption process

A solution of Cd^{+2} with a concentration of 500 mg/L was prepared. Different amounts (20–100 mg/l) of cadmium ions concentration were added to a conical flask that already had 0.1 g of modified zeolite nanocomposites and 0.3 g of alumina as an adsorbent, then it was put in a vibrating water bath that was kept at a constant temperature of 293 K. After shaking for required times, the solutions were centrifuged at 4000 rpm for 15 minutes and then filtered to get rid of the ions that stuck to the surface. The quantity of adsorbed ions and removal was determined using Equation (1 and 2), where qe_{ion} denotes the amount of adsorbed ions of cadmium (mg/g), C_i indicates the initial amount of ions (mg/L) in solution, C_f

signifies the final concentration of ions (mg/L), V_{sol} represents the volume of Cd(II) ions solution, and M is the mass of the adsorbent, $R_{ion}\%$ is percentage ions removal [28].

$$qe_{ion} = \frac{(C_i - C_f)\, V_{sol}}{M} \qquad \text{Eq.1}$$

$$R_{ion}\% = \frac{(C_i - C_f)}{C_i}\, x\, 100 \qquad \text{Eq.2}$$

2.4. Simulations of adsorption using mathematical isotherms

The effectiveness of cadmium ion adsorption was assessed utilising five distinct isothermal models: Langmuir, Freundlich, Timken, Dubinin, and Harken-Jura: In this equation, C_{eq} represents the concentration of ions at equilibrium, (q_m and k_L) are the Langmuir coefficients, and qe_{ion} represents the amount of adsorption which is present at equilibrium[29].

$$\frac{C_{eq}}{qe_{ion}} = \frac{1}{q_m k_L} + \frac{C_{eq}}{q_m} \qquad Eq.3$$

The Freundlich isotherm applies to systems exhibiting a heterogeneous surface, characterised by the heterogeneity constant (1/n). The linear representation of the model is as follows [30]: K_f denotes the Freundlich constant.

$$log\ qe_{ion} = log\ K_f + \frac{1}{n} log\ C_{eq} \qquad \text{Eq.4}$$

The Temkin isotherm model is predicated on robust electrostatic interactions, with k_T representing the variation in adsorption energy. The heat of adsorption for all molecules in the layer is supposed to decrease linearly with increasing coverage [31]: B pertains to the heat of adsorption. $B = \frac{RT}{b}$, where T is the absolute temperature (K), R is (8.314 J mol^{-1} K^{-1}), b signifies the Temkin constant.

$$qe_{ion} = B ln\ k_T + B\ ln C_{eq} \qquad \text{Eq.5}$$

In the case where the adsorbed layer is of the condensed type, the Harkins-Jura adsorption isotherm (Eq.6), which was initially formulated for gas-solid systems, is applicable to solution-solid systems as well [32]. Where A and B are the Harkins model constants.

$$\frac{1}{eq_{ion}^{2}} = \left[\frac{B}{A}\right] - \left[\frac{1}{A}\right] logC_{eq} \qquad Eq.6$$

3. Results and discussion

3.1. Sorbents characterization

The distinctions between spherical alumina and zeolite alumina nanocomposites regarding surface area, pore volume, and pore diameter are encapsulated in Table 1. Mesoporous alumina is found favoured as an adsorbent due to its elevated surface area, compared to zeolite nanocomposite. From the values mentioned in Table 1, the surface of spherical alumina has the highest surface area, reaching (193.75 $m^2. g^{-1}$) with the pore volume (0.373$cm^3. g^{-1}$) according to the BET theory and the average of pore diameter is (7.693 nm) according to the BJH isotherm. On the other hand, the zeolite nanocomposite has low surface area (134.24 $m^2. g^{-1}$), the low pore volume (0.207$cm^3. g^{-1}$), and its average pore diameter is (6.20 nm). From the pore diameter measurements of the two surfaces, the surfaces are of the mesoporous type according to the categorisation established by the International Union of Pure and Applied Chemistry [33, 34] for porous solids that have a pore diameter range between (2-50) nm.

Table 1. Specific area of adsorbents, pore volume, and pore diameter.

Adsorbents	Surface area (m^2/g)	pore volume (cm^3/g)	Pore diameter (nm)
alumina nanoparticle	193.75	0.373	7.693
zeolite-alumina composite	134.24	0.207	6.201

The crystalline structure of adsorbents was analysed using X-ray diffraction. (XRD) analysis of the zeolite nanocomposite revealed three broad peaks and three

sharp peaks with high intensity, indicating the presence of oxide combinations and the creation of the new compound. Figure 1 shows the angles and relative intensities of the absorption peaks for each of the adsorbents separately. The d values that got from X-ray diffraction were compared to those on standard table cards in the ICDD database. This indicated that silicon oxide (SiO□) peak at 2 θ=29.23, which has a hexagonal crystal structure, is the main inorganic crystalline material on the surface of the zeolite. As well as the presence of a crystal structure of calcium alumina silicate 8CaAl□Si□O on the surface nanocomposite [35]. Figure 1 A displays the XRD pattern of alumina, with the highest-intensity peaks of the phase composed of sodium aluminium silicate indexed at 31, 37.5, 39.4, 45.92, 60.7 and 66.97 degrees. The X-ray diffraction pattern of the synthesised zeolite nanocomposite is depicted in Figure 1B with diffraction peaks at 38.2, 46.5, and 68.9 [JCPDS No. 04-0787] indicating the presence of aluminium metal and diffraction peaks at 37.6, 47.8 [JCPDS No.10-0425] showing the formation of Al-O phase indicating the presence of Al_2O_3 [36]. Based on the X-ray diffraction peaks and the Scherrer equation (Eq.7) [37], the crystallite diameters of alumina and zeolite nanocomposite were found to be 4.58 nm and 6.47 nm, respectively.

$$D = \frac{0.9\lambda}{\beta.COS\ \theta} \qquad \text{Eq.7}$$

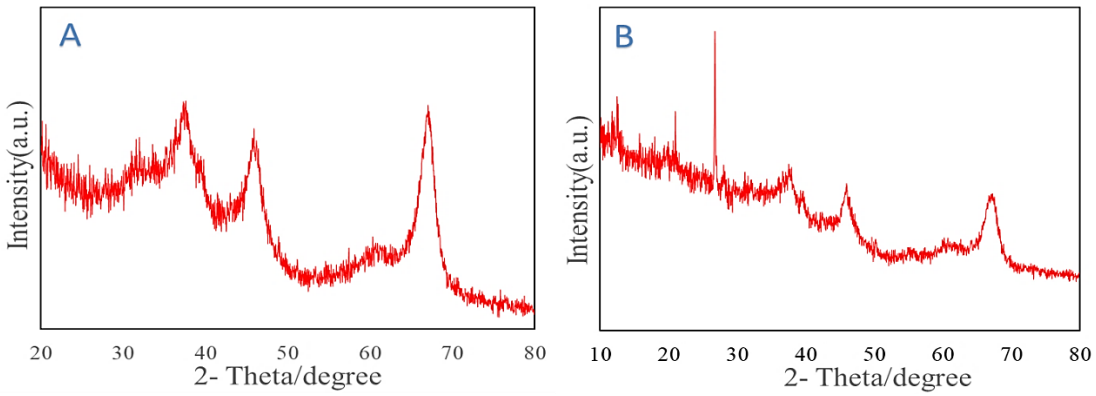

Figure1. XRD-diffraction pattern of (A) alumina and (B) zeolite-alumina nanocomposite.

Energy-dispersive X-ray (EDX) was employed to determine the atomic and weight ratios of the elements present on the adsorbents, as shown in Figure 2. The analysis

showed a significant increase in the oxygen content of the surfaces due to the improvement from the presence of alumina and silicon oxides; this outcome is consistent with previous studies [38].

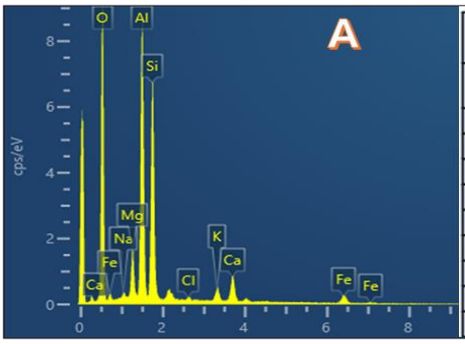

zeolite alumina nanocomposite			Spherical alumina nanoparticles		
El.	Wt.%	At%	El.	Wt.%	At%
C	1.24	5.28	C	9.38	15.01
O	50.46	54.07	O	44.16	53.05
Na	0.47	0.42	Na	0.27	0.23
Al	27.63	22.80	Mg	1.11	0.87
Si	13.36	12.6	Al	34.79	24.78
Mg	2.35	1.49	Si	6.62	4.53
Ca	2.04	1.68	K	0.61	0.30
Fe	1.13	1.12	Ca	1.24	0.60
K	1.32	0.54	Fe	1.82	0.63

Figure 2. Elemental analysis of alumina and zeolite alumina nanocomposite A

Understanding the morphological differences between alumina and zeolite-alumina nanocomposite is crucial for improving their effectiveness in adsorption applications. The sorbents have a heterogeneous porous structure, as depicted in Figure 3A, which characterizes the alumina sorbent as a non-uniform amalgamation of pore geometries [39]. Conversely, Figure 3B depicts the existence of metal oxide on the surfaces of the zeolite alumina nanocomposites, distinguished by the most pronounced wrinkles.

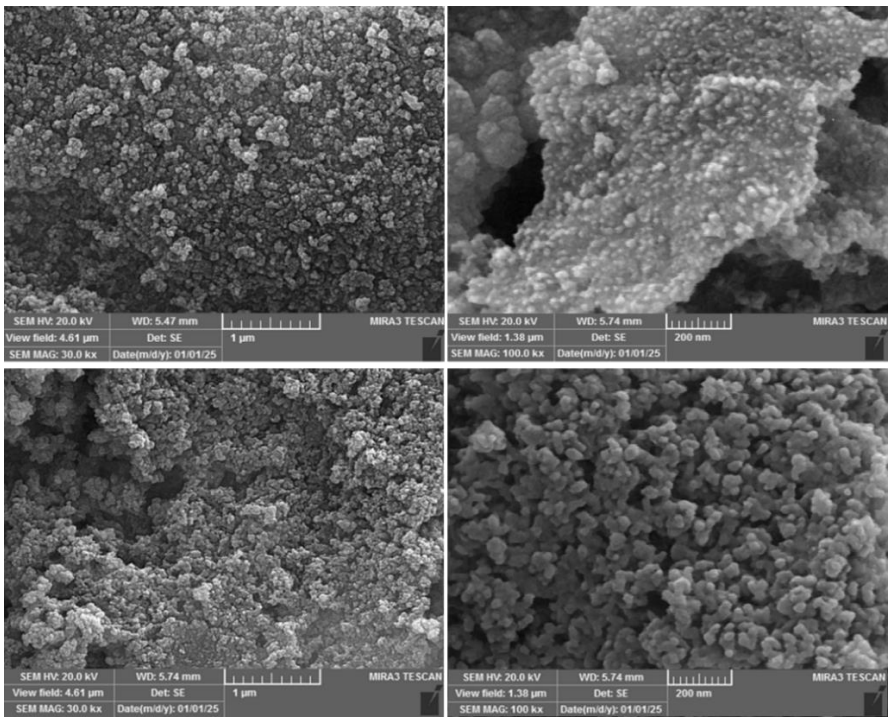

Figure3. SEM images of (A) alumina and (B) zeolite alumina nanocomposite at different magnifications.

The absorbents were analysed spectroscopically via infrared spectroscopy, with measurements conducted at ambient temperature. The data indicated adsorption maxima within the region of 400-4000 cm□¹. This spectral area encompasses numerous significant stretching modes, including those of carbon, hydrogen, oxygen, and alumina. The spectra below 1000 cm^{-1} illustrate the fundamental properties of alumina. A broad range ranging from 3700 to 3100 cm□¹, with the acid sites Si-OH–Al (Brønsted site) centred at 3448 cm□¹ [40]. The initial peak at 443 cm□¹ was attributed to Al-O or Si-O buckling vibrations. At the second high of 565 cm□¹, T-O-T (T = Al or Si) bonds in five-membered rings exhibited unequal stretching [41]. The various valence vibrations of the (Si, Al)–O bond result in the absorption bands shifting at 1015cm^{-1} [42]. Hydrated aluminosilicates exhibit stretching and bending absorption bands for OH groups at 3700 -1100 cm^{-1} and 1655 cm^{-1}, respectively [43].

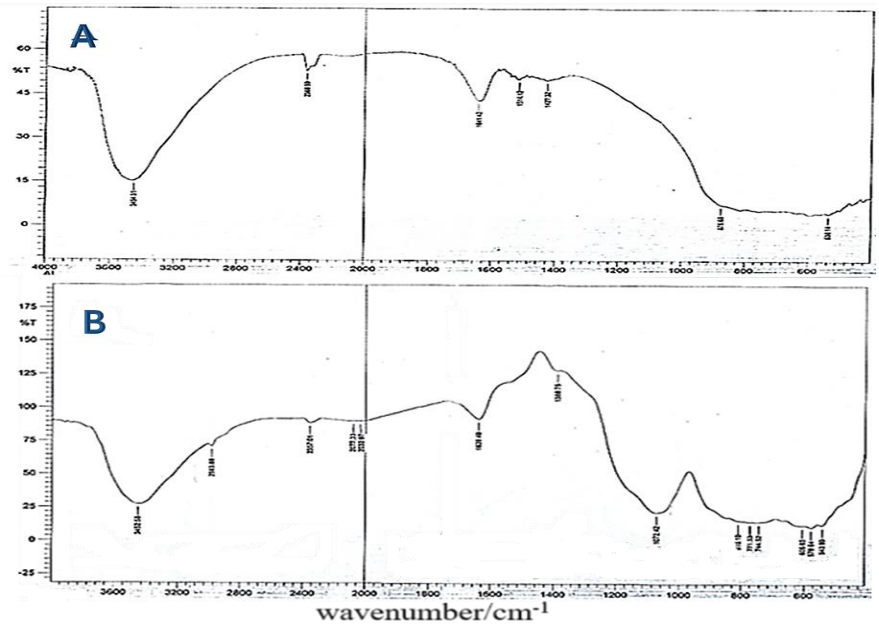

Figure 4. FT-IR analysis of alumina A and zeolite alumina nanocomposite B.

3.2. Batch adsorption investigations for the removal of Cadmium ions

3.2.1 weight of the adsorbents, the contact time, and pH value.

The influence of adsorbent mass on cadmium ion concentration was assessed. A 25 mL solution of cadmium ions at a concentration of 40 mg/L was prepared and mixed with different weights of surfaces, ranging from 0.05 g to 2 g. Figure 5 illustrates that an increase in adsorbent weight modifies the surface uptake. The ideal explanation is the presence of several active sites and the resulting increased surface-to-volume ratio [44]. Moreover, beyond a certain quantity of each adsorbent, there has been no improvement in the removal efficiency of cadmium ions. This may be because the surface is saturated with adsorbate molecules, resulting in no observable effect with an increase in adsorbent dose. So, the best weights for alumina, and zeolite-alumina composite surfaces are 0.3 g, and 0.1 g, respectively. However, increasing the adsorbent dose by more than 0.3 g, results in a decrease in the metal ion uptake. An excessive dosage of the adsorbent might cause aggregation, leading to a decrease in active sites; thus, the overall surface area of the adsorbent material is reduced, and the diffusional path length is extended [45]. As cadmium ions adsorb onto the spherical alumina, it was seen that the amount of adsorption goes up as the amount of adsorbent goes up until it reaches a certain weight (0.3 g). This may be due to the presence of a few effective sites on the surface at low weight of the adsorbent material and thus leads to the possibility of the adsorbent material binding to the adsorbent surface being weak due to the limited number of sites existing on the surface [46].

The time of equilibrium is also examined. A suitable quantity of each surface of a 40 mg/L cadmium concentration was combined for 10 to 100 minutes at 20°C. Figure 5 illustrates that the efficacy of removal increases with prolonged contact time, ultimately achieving removal percentages of 92.5% for alumina and 90% for the zeolite-alumina composite.

According to pH value, the results indicate that adsorption on examined surfaces rises with concentration, peaking at pH= 6. This effect is due to the significant

probability of electrostatic attraction between the cadmium cation and the negative surface charge. The elevated value of the acidic function will increase the hydroxide ion and induce negative charges on the surface, hence enhancing the extent of adsorption. When the pH level reached 6, the zeolite alumina-silicate (Al-Si–O) structure system [47] could remove up to 90% of the Cd (II) ions and 92.5% of them from the zeolite composite and alumina, with multilayer adsorption capacities of 8.95 mg/g and 3.07 mg/g, respectively.

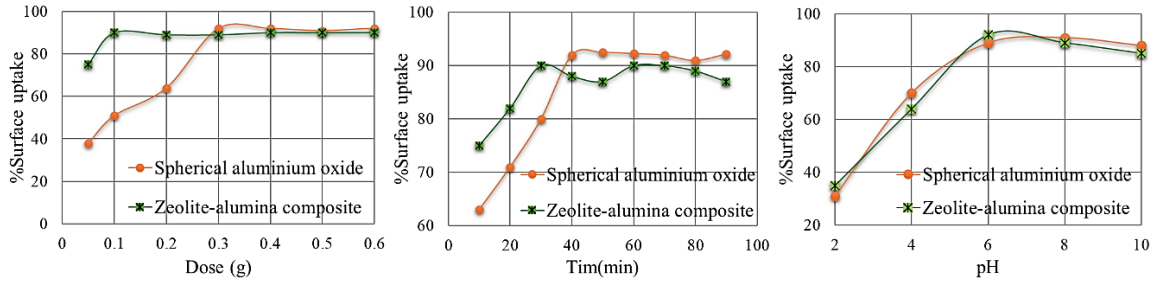

Figure 5. The effect of the adsorbents weight, contact time and pH on Cd (II) removal

3.2.2. Adsorption of Cadmium ions isotherms

Isotherms serve to characterise interactions between adsorbates and adsorbents. Five significant isotherm models, specifically Langmuir, Freundlich, Temkin, and Harken-Jura, were evaluated for their ability to fit the experimental adsorption data (figures 6 and7). The evaluation of adsorption onto sorbents was conducted by comparing their respective R^2 values. The experimental results were evaluated across the selected models, revealing that the experimental equilibrium data of sorbents exhibited a strong correlation with the Freundlich and Temkin isotherms, as confirmed by the highest R^2 value. The adsorption surfaces exhibit heterogeneity with multilayer coverage until the saturation of active sites is reached on both adsorbents. As can be seen from Figure 7, based on the B values for alumina (0.326) and zeolite alumina composite (0.1), the Temkin adsorption model says that the heat of adsorption went down during the sorption process [48], which is in line with thermodynamic values. In contrast, the Langmuir model, which asserts homogeneous monolayer adsorption, yielded an R^2 value of 0.426

for the zeolite alumina, which is lower than the R^2 values for the Freundlich adsorption models, indicating the presence of heterogeneous multilayer adsorption.

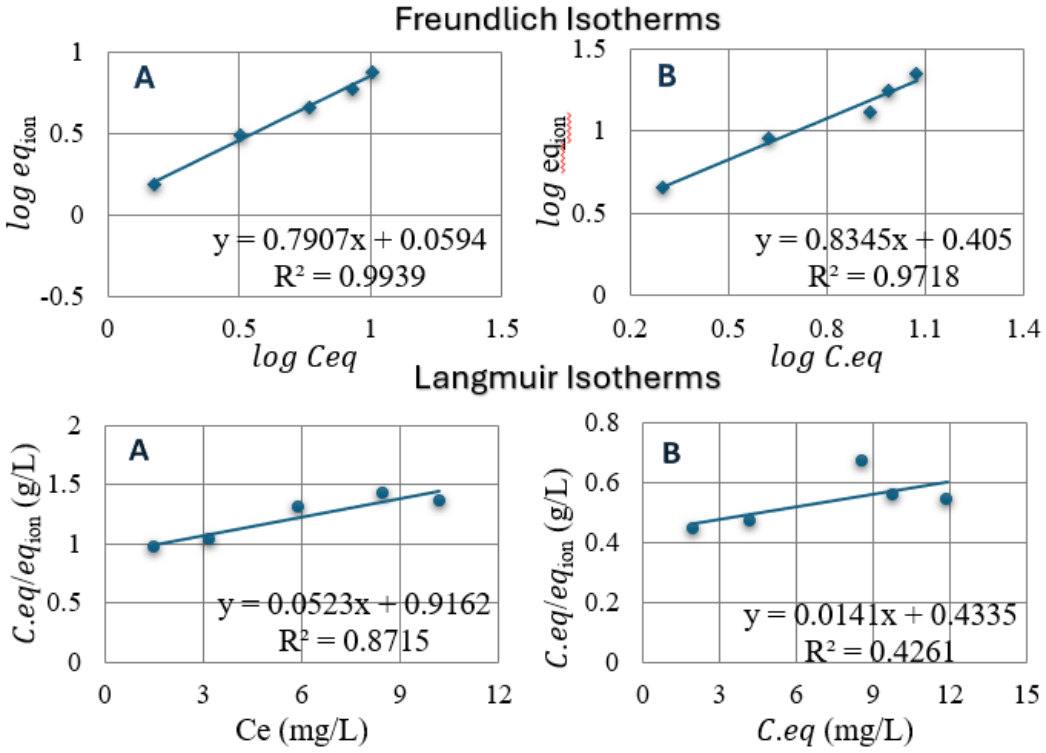

Figure 6. Freundlich and Langmuir straight lines for adsorption of Cd (II) by alumina (A) and zeolite alumina nanocomposite (B) at pH=6, and 293 K.

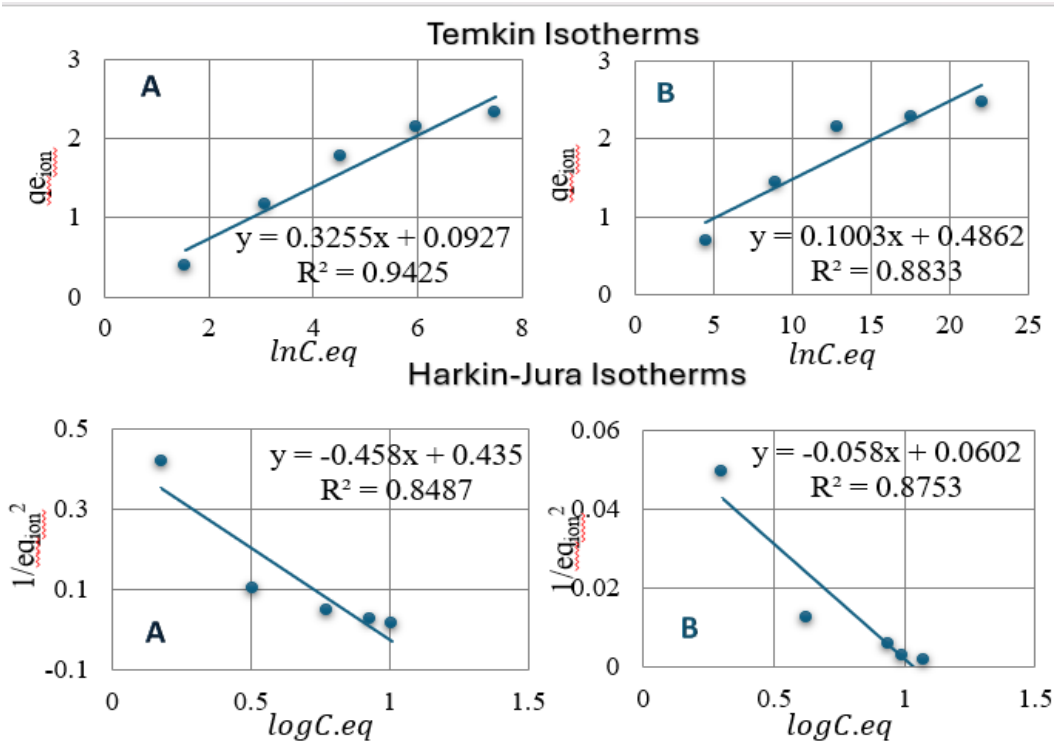

Figure 7. Temkin and Harkin-Jura straight lines for adsorption of Cd (II) by alumina (A) and zeolite alumina nanocomposite (B) at pH=6, and 293 K.

Three different temperatures (293, 303, 313) K is explained the adsorption trend as shown in Figure 8. Zeolite alumina nanocomposite exhibited high ions adsorption capacities, likely attributable to its porous structure and elevated surface area, which may facilitate the availability of additional adsorption sites, hence enhancing the adsorption capacity [49]. These results of enhancement in adsorption uptake with increasing adsorbate concentration align with prior investigations conducted by Yan et al. [50]. It has been also observed that Cd ions adsorption increases by increasing the temperature on alumina in contrast on zeolite alumina composite.

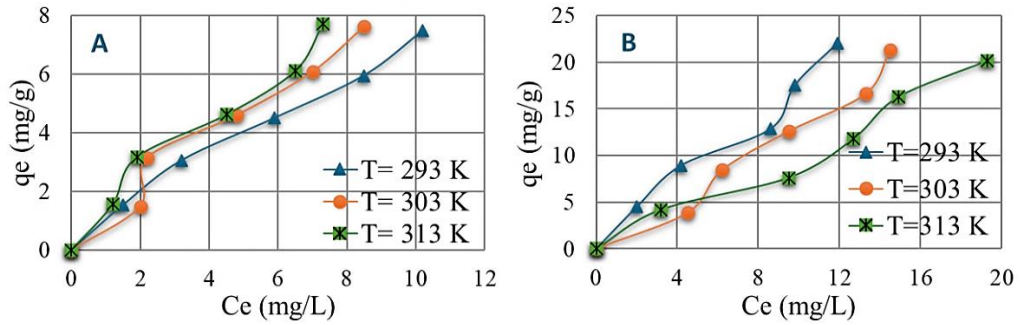

Figure 8. Temperature effect of Cd (II) adsorption by alumina (A) and zeolite alumina nanocomposite (B) at pH=6.

3.2.3 Thermodynamic Functions calculation

The thermodynamic parameters, including enthalpy, Gibbs free energy, and entropy variations, were computed adsorption of Cd (II) and presented in the table 3. The value at each temperature was computed using the following vant Hoff equation to determine the values of enthalpy (ΔH) and entropy (ΔS) as presented in it [51]. The equilibrium constant (Kequ.) serves to examine the thermodynamic parameters, with the alteration in Gibbs free energy of adsorption represented by Equation 9 and 10 [52].

$$Ln\ Kequ. = -\frac{\Delta H^{\circ}}{RT} + \frac{\Delta S^{\circ}}{R} \qquad Eq.8$$

$$Ln\ Kequ. = \frac{Q_{eq} * M}{C_{eq} * V} \qquad Eq.9$$

$$\Delta G^{\circ} = -RT\ Ln\ Kequ. \qquad Eq.10$$

The adsorbent surface's dose is represented by M (g). V (L) represents the volume of the solution. R is constant (8.314 J mol^{-1} K^{-1}); The values of ΔH° and ΔS° can be determined from the slope and intercept, respectively, of the linear plot of ln Kequ. vs 1/T. In Table 3, the negative value of ΔG signifies the feasibility and spontaneity of the adsorption process on adsorbents under study. A positive value of ΔH indicates that the adsorption of cadmium ions onto alumina was endothermic in contrast on modified Zeolite nanocomposite was exothermic. An increase in temperature elevates the kinetic energy of the ions adhered to the adsorbent surface, resulting in reduced mobility of the adsorbate molecules on the adsorbent surface, thereby weakening the attractive forces between the cadmium ions and the active sites on the surface [53]. Furthermore, the negative value of ΔS signifies a reduction in randomness and a decrease in the degrees of freedom of the adsorbed ions, indicating that the ions are constrained by the adsorbent surface, resulting in a more ordered arrangement; hence, the type of adsorption is physisorption. The negative value of ΔG◦ with rising temperature signifies the

feasibility and spontaneous nature of adsorption, which becomes increasingly spontaneous at higher temperatures [54].

Table 3. Thermodynamic parameters for adsorption of Cd (II) onto sorbents at Temp=293 K.

Absorbent surfaces	Thermodynamic functions		
	ΔH kJ/mol	ΔG kJ/mol	ΔS J/mo1. k
Spherical aluminium oxide	$+13.974x10^{-3}$	-5.299	$+65.811$
Zeolite-alumina composite	$-21.724x10^{-3}$	-4.877	-57.316

Conclusion

This study aimed to examine eliminating Cd (II) ions using two different adsorbents: spherical alumina and zeolite-alumina nanocomposite. The study showed that a modified zeolite nanocomposite made using the hydrothermal calcination method can effectively adsorb cadmium ions because it makes aluminosilicate nanocomposites with a lot of surface area. Maximum removal efficiencies of 92.5% and 90% were observed for alumina and modified zeolite nanocomposite, respectively demonstrating its potential for practical applications in wastewater treatment. Optimal Cd(II) removal by both adsorbents occurred at pH 6. The isotherm analysis indicated that the Freundlich and Temkin models were better at explaining ion adsorption on alumina than the modified one due to a higher R^2 value. Adsorption isotherms typically fit the Freundlich model best, with maximum adsorption capacities ranging from 7.48 mg/g for alumina to 22.03 mg/g for zeolite-alumina nanocomposite. When the temperature is raised from 293 K to 313 K, the alumina's maximum Cd (II) adsorption capacity goes up from 7.48 mg/g to 7.73 mg/g. On the other hand, the zeolite nanocomposite's maximum Cd (II) adsorption capacity goes down from 22.03 mg/g to 20.18 mg/g.

Thermodynamic studies revealed that adsorption processes were spontaneous, with varying endothermic or exothermic nature depending on the adsorbent.

References

[1] Singh, V. [2024]: Textbook of Environment and Ecology, Springer, pp. 217-224, doi: 10.1007/978-981-99-8846-4.

[2] Thrikkaikkal, H., & Harikumar, P. S. [2024]: Role of Nanotechnology in the Remediation of Heavy Metals. In Heavy Metal Toxicity: Human Health Impact and Mitigation Strategies, Cham: Springer Nature Switzerland, pp. 357-383.

[3] Alsharif, N. B., Muráth, S., Katana, B., & Szilagyi, I. [2021]: Composite materials based on heteroaggregated particles: Fundamentals and applications. Advances in Colloid and Interface Science, 294, 102456, doi: 10.1016/j.cis.2021.102456.

[4] Khan, S., & Şengül, H. [2016]: Experimental investigation of stability and transport of TiO2 nanoparticles in real soil columns. Desalination and Water Treatment, 57(54), 26196-26203, doi:10.1080/19443994.2016.1163513.

[5] Khan, S., Şengül, H., & Dan, Z. [2018]: Transport of TiO2 nanoparticles and their effects on the mobility of Cu in soil media. Desalination and Water Treatment, 131, pp. 230-237. doi:10.5004/dwt.2018.22952.

[6] Bayar J. et al., [2024]: Biochar-based adsorption for heavy metal removal in water: a sustainable and cost-effective approach, Environ. Geochem. Health, vol. 46, no. 11, pp. 1–25, doi: 10.1007/s10653-024-02214-w.

[7] Rajendran, S., Priya, A. K., Kumar, P. S., Hoang, T. K., Sekar, K., Chong, K. Y., ... & Show, P. L. [2022]: A critical and recent developments on adsorption technique for removal of heavy metals from wastewater-A review. Chemosphere, 303, 135146, doi: 10.1016/j.chemosphere.2022.135146.

[8] Nworie F. S., [2024]: Development of Nano-adsorbent for Heavy Metals Removal from Wastewater, Springer Nature Switzerland, vol. Part F3243.

[9] Wawata, I. G., & Fabiyi, O. A. [2024]: Sustainable application of nanomaterials in the removal of heavy metals from water. In Sustainable

Nanomaterials: Synthesis and Environmental Applications, Singapore: Springer Nature Singapore. pp. 21-44, doi:10.1007/978-981-97-2761-2_2.

[10] Yimer M. et al., [2024]: Adsorptive removal of heavy metals from wastewater using Cobalt-diphenylamine (Co-DPA) complex, BMC Chem., vol. 18, no. 1, pp. 1–15, doi: 10.1186/s13065-024-01128-z.

[11] Roy, S., & Ahmaruzzaman, M. [2022]: Ionic liquid-based composites: A versatile material for remediation of aqueous environmental contaminants. Journal of Environmental Management, 315, 115089.

[12] Su, H. et al. [2024]: Low-silica zeolite MTT: synthesis and efficient catalysis in methanol dehydration. Microporous Mesoporous Mater. 378, 113268.

[13] Khivantsev, K., Derewinski, M. A. & Szanyi, [2023]: J. Novel and emerging concepts related to cationic species in zeolites: characterization, chemistry and catalysis. Microporous Mesoporous Mater. 358, 112378, doi: 10.1016/j.micromeso.2022.112378.

[14] Weitkamp, [2000]: J. Zeolites and catalysis. Solid State Ionics. 131, 175–188, doi:10.1016/S0167-2738(00)00632-9.

[15] Corma, A. [2003]: State of the art and future challenges of zeolites as catalysts. J. Catal. 216, pp. 298–312, doi:10.1016/S0021-9517(02)00132-X.

[16] Caputo, D. & Pepe, F. [2007]: Experiments and data processing of ion exchange equilibria involving Italian natural zeolites: a review. Microporous Mesoporous Mater. 105, pp. 222–231, doi: 10.1016/j.micromeso.2007.04.024.

[17] Cheng, H. et al. [2023]: Application of unconventional external-field treatments in air pollutants removal over zeolite-based adsorbents/catalysts. Catalysts 13, 1461, doi.org/10.3390/catal13121461.

[18] Margeta, K., Logar, N. Z., Šiljeg, M. & Farkaš, A. [2013]: Natural zeolites in water treatment–how effective is their use. Water Treat. 5, pp. 81–112, doi.org/10.5772/50738.

[19] Wang, S. & Peng, Y. [2010]: Natural zeolites as effective adsorbents in water and wastewater treatment, Chem. Eng. J. 156, pp. 11–24, doi: 10.1016/j.cej.2009.10.029.

[20] Lu, W. et al. [2022]: Research progress of modified natural zeolites for removal of typical anions in water, Environ. Science: Water Res. Technol. 8, pp. 2170–2189, doi: 10.1039/D2EW00478J.

[21] Rad, L. R. & Anbia, M. [2021]: Zeolite-based composites for the adsorption of toxic matters from water, a review. J. Environ. Chem. Eng. 9, 106088, doi: 10.1016/j.jece.2021.106088.

[22] Lu, P. et al. [2024]: A stable zeolite with atomically ordered and interconnected mesopore channel, Nature, vol. 636, no. 8042, pp. 368–373, doi: 10.1038/s41586-024-08206-1.

[23] Jafari, B., Rezaei, E., Abbasi, M., Hashemifard, S. A., & Sillanpää, M. [2022]: Application of mullite-zeolite-alumina microfiltration membranes coated by SiO2 nanoparticles for separation of oil-in-water emulsions. Journal of the European Ceramic Society, 42(13), 6005-6014, doi: 10.1016/j.jeurceramsoc.2022.06.060.

[24] Jadhav, P. et al. [2007]: Monoethanol amine modified zeolite 13X for CO2 adsorption at different temperatures. Energy Fuels. 21, 3555–3559.

[25] Başkan, G., Açıkel, Ü. & Levent, M. [2022]: Investigation of adsorption properties of oxytetracycline hydrochloride on magnetic zeolite/Fe3O4 particles. Adv. Powder Technol. 33, 103600, doi: 10.1016/j.apt.103600.

[26] Šljivić, M., Smičiklas, I., Pejanović, S. & Plećaš, I. [2009]: Comparative study of Cu2 + adsorption on a zeolite, a clay and a diatomite from Serbia, Appl. Clay Sci. 43, pp. 33–40, doi: 10.1016/j.clay.2008.07.009.

[27] Khan, S., Galstyan, H., Ahmed Bazai, N., & Idrees, M. [2022]: Surface interaction of cadmium and zinc metal ions on Al2O3 nanoparticles in aqueous solution, International Journal of Environmental Analytical Chemistry, 102(17), pp. 5321-5338.

[28] Mushtaq, N., Munir, R., Zia-ur-Rehman, M., ul-Haq, Z., Bashir, M. Z., Muneer, A., ... & Noreen, S. [2024]: Construction and utilization of innovative zeolite/perovskite/graphene oxide, zeolite/chitosan/graphene oxide, and zeolite/biochar/graphene oxide nanohybrid composites for adsorptive remediation of cationic dye from wastewater, Water Conservation Science and Engineering, 9(1), 33, doi:10.1007/s41101-024-00264-w.

[29] Mabuza, M., Premlall, K., & Daramola, M. O. [2022]: Modelling and thermodynamic properties of pure CO2 and flue gas sorption data on South African coals using Langmuir, Freundlich, Temkin, and extended Langmuir isotherm models. International Journal of Coal Science & Technology, 9(1), 45.

[30] Chen, X., Hossain, M. F., Duan, C., Lu, J., Tsang, Y. F., Islam, M. S., & Zhou, Y. [2022]: Isotherm models for adsorption of heavy metals from water-A, review. Chemosphere, 307, 135545, doi: 10.1016/j.chemosphere.2022.135545.

[31] Mahanty, B., Behera, S. K., & Sahoo, N. K. [2023]: Misinterpretation of Dubinin–Radushkevich isotherm and its implications on adsorption parameter estimates, Separation Science and Technology, 58(7), pp.1275-1282.

[32] Yılmaz, D., Gürses, A., Kalecik, S., Maman, A., Şahin, E., & Güneş, K. [2024]: Removal of 177Lu from radioactive wastewater using Montmorillonite clay, Applied Radiation and Isotopes, 211, 111417, doi: 10.1016/j.apradiso.111417.

[33] Lowell, S., Shields, J. E., Thomas, M. A., & Thommes, M. [2012]: Characterization of porous solids and powders: surface area, pore size and density, Springer Science & Business Media. (Vol. 16).

[34] Villarroel-Rocha, J., Barrera, D., Arroyo-Gómez, J. J., & Sapag, K. [2020]: Critical overview of textural characterization of zeolites by gas adsorption. New Developments in Adsorption/Separation of Small Molecules by Zeolites, pp. 31-55, doi:10.1007/430_2020_69.

[35] Caputo, D., Liguori, B., & Colella, C. [2008]: Some advances in understanding the pozzolanic activity of zeolites: The effect of zeolite structure, Cement and Concrete Composites, 30(5), pp. 455-462.

[36] Al-Gaashani, R., Alyasi, H., Karamshahi, F., Simson, S., Tongb, Y., Kochkodan, V., & Lawler, J. [2024]: Nickel removal from synthetic wastewater by novel zeolite-doped magnesium-iron-and zinc-oxide nanocomposites by hydrothermal-calcination technique, Scientific Reports, 14(1), 30954, doi: 10.1038/s41598-024-81947-1.

[37] Hassanzadeh-Tabrizi, S. A. [2023]: Precise calculation of crystallite size of nanomaterials, A review. Journal of Alloys and Compounds, 968, 171914, doi: 10.1016/j.jallcom.2023.171914.

[38] Mardkhe, M. K., Keyvanloo, K., Bartholomew, C. H., Hecker, W. C., Alam, T. M., & Woodfield, B. F. [2014]: Acid site properties of thermally stable, silica-doped alumina as a function of silica/alumina ratio and calcination temperature, Applied Catalysis A: General, 482, pp.16-23, doi.org/10.1016/j.apcata.2014.05.011.

[39] Wu, J., Zhu, X., Yang, F., Wang, R., & Ge, T. [2022]: Shaping techniques of adsorbents and their applications in gas separation, a review, Journal of Materials Chemistry A, 10(43), pp. 22853-22895, doi.org/10.1039/D2TA04352A.

[40] Kowenje, C. B. [2006]: Spectroscopic characterization of the metal cation siting and the adsorbate-cation interactions in copper (II) and cobalt (II) exchanged faujasite-X zeolite, State University of New York at Binghamton.

[41] H. Liu, Y. Wang, H. Yuan, and W. Luo, [2024]: Synthesis of Nanoscale ZSM-5 Zeolites for the Catalytic Cracking of Oleic Acid into Light Olefins and Aromatics, J. Inorg. Organomet. Polym. Mater., no. 0123456789x, doi: 10.1007/s10904-024-03404-w.

[42] Abdeldaym, A., Sallam, O. I., Ezz-Eldin, F. M., & Elalaily, N. A. [2021]: Influence of gamma irradiation on the optical, thermal and electrical features of

blue commercial glass as potential accident dosimetry, Journal of Physics and Chemistry of Solids, 157, 110196, doi: 10.1016/j.jpcs.2021.110196.

[43] Slaný M., Kuzielová E., Žemlička M., Matejdes M., Struhárová A., and Palou M. T., [2023]: Metabentonite and metakaolin-based geopolymers/zeolites: relation between kind of clay, calcination temperature and concentration of alkaline activator, J. Therm. Anal. Calorim., vol. 148, no. 20, pp. 10531–10547, doi: 10.1007/s10973-023-12267-1.

[44] Sinbah, H., Khazaal, M., & Majeed, N. [2021]: Isotherms, Kinetics and Thermodynamic Studies for Removal the Valium from Stomach and Intestine Fluids via Adsorption on Egg Shells Powder, Indian Journal of Forensic Medicine & Toxicology, 15(1).

[45] Tony, M. A., Parker, H. L., & Clark, J. H. [2019]: Evaluating Algibon adsorbent and adsorption kinetics for launderette water treatment: towards sustainable water management. Water and Environment Journal, 33(3), pp. 401-408, doi: 10.1111/wej.12412.

[46] Chakraborty, R., Asthana, A., Singh, A. K., Jain, B., & Susan, A. B. H. [2022]: Adsorption of heavy metal ions by various low-cost absorbents, a review. International Journal of Environmental Analytical Chemistry, 102(2), pp. 342-379, doi:10.1080/03067319.2020.1722811.

[47] Wahono, S. K., Stalin, J., Addai-Mensah, J., Skinner, W., Vinu, A., & Vasilev, K. [2020]: Physico-chemical modification of natural mordenite-clinoptilolite zeolites and their enhanced CO2 adsorption capacity, Microporous and Mesoporous Materials, 294, 109871, doi: 10.1016/j.micromeso.2019.109871.

[48] Lu, L., & Na, C. [2022]: Gibbsian interpretation of Langmuir, Freundlich and Temkin isotherms for adsorption in solution, Philosophical Magazine Letters, 102(7), pp. 239-253, doi:10.1080/09500839.2022.2084571.

[49] Tony, M. A. [2020]: Zeolite-based adsorbent from alum sludge residue for textile wastewater treatment, international journal of environmental science and technology, 17(5), pp. 2485-2498, doi: 10.1007/s13762-020-02646-8.

[50] Yan, S., Cai, Y., Li, H., Song, S., & Xia, L. [2019]: Enhancement of cadmium adsorption by EPS-montmorillonite composites, Environmental Pollution, 252, pp. 1509-1518, doi: 10.1016/j.envpol.2019.06.071.

[51] Shenjin, W., Xiaoxi, L., Chenyang, Z., Wenjihao, H., Yaochi, L., Xinzhuang, F., ... & Wei, S. [2025]: Adsorption and selective mechanism of Pb2+ and Cd2+ on the surface of calcined modified attapulgite, Separation and Purification Technology, 353, 128377, doi: 10.1016/j.seppur.2024.128377.

[52] Ortiz-Oliveros, H. B., Ouerfelli, N., Cruz-Gonzalez, D., Avila-Pérez, P., Bulgariu, L., Flaifel, M. H., & Abouzeid, F. M. [2023]: Modeling of the relationship between the thermodynamic parameters ΔH° and ΔS° with temperature in the removal of Pb ions in aqueous medium, Case study. Chemical Physics Letters, 814, 140329, doi: 10.1016/j.cplett.2023.140329.

[53] Bhutto, A. A., Baig, J. A., Kazi, T. G., Sierra-Alvarez, R., Akhtar, K., Perveen, S., ... & Samejo, S. [2023]: Biosynthesis of aluminium oxide nanobiocomposite and its application for the removal of toxic metals from drinking water, Ceramics International, 49(9), pp. 14615-14623, doi: 10.1016/j.ceramint.2023.01.052.

[54] Hassan, H. S., Madcour, W. E., & Elmaghraby, E. K. [2019]: Removal of radioactive cesium and europium from aqueous solutions using activated Al2O3 prepared by solution combustion, Materials Chemistry and Physics, 234, pp. 55-66, doi: 10.1016/j.matchemphys.2019.05.081.